

# Investigation of the electronic mechanism of the isomorphous phase transition in cerium

V. A. Shaburov, I. M. Band, A. I. Grushko, T. B. Mezentseva, E. V. Petrovich, Yu. P. Smirnov, A. E. Sovestnov, O. I. Sumbaev, M. B. Trzhaskovskaya, and I. A. Markova

Nuclear Physics Institute, USSR Academy of Sciences

(Submitted March 30, 1973)

Zh. Eksp. Teor. Fiz. 65, 1157-1174 (September 1973)

The  $\gamma$ -cerium- $\alpha$ -cerium isomorphous phase transition<sup>[1-8]</sup> is investigated experimentally by the technique of chemical shifting of x-ray lines.<sup>[15, 16]</sup> The transition was induced in pure metallic cerium samples by cooling to nitrogen-helium temperatures and by high effective pressures in lattices of the so-called Laves phases at room temperature. Characteristic changes in energy of the x-ray ( $K_{\alpha 1}$ ,  $K_{\beta 1}$ ,  $K_{\beta 2, 4}$ ) lines are observed during the  $Ce_{\gamma}$ - $Ce_{\alpha}$  transition and are similar to those observed in comparing trivalent ( $Ce^{III}$ ) and quadrivalent ( $Ce^{IV}$ ) cerium. Self-consistent calculations according to Hartree-Fock-Slater with Wigner-Seitz boundary conditions are carried out. It is found that the  $Ce_{\gamma}$ - $Ce_{\alpha}$  transformation undoubtedly involves a decrease of the number of collapsed 4f electrons. The reduction in the number 4f electrons in this case comprises about half of that observed in the  $Ce^{III}$ - $Ce^{IV}$  transition. The absolute value depends on the assumptions regarding the electron configurations of  $Ce^{III}$  and  $Ce^{IV}$  and lies between 1/4 and 1/2 4f electron per atom, the values near to 1/2 being more probable.

## INTRODUCTION

The first-order phase transition in metallic cerium, which occurs at room temperature and a pressure  $p \approx 7$  kbar<sup>[1]</sup> or at normal ( $p \approx 0$ ) pressure and low temperatures ( $T \leq 160^\circ K$ )<sup>[2]</sup>, is unique. It is not accompanied by a change in the lattice symmetry and has been called isomorphous. ( $\gamma$  cerium is stable at normal pressure and temperature, and its FCC lattice experiences only a similar compression on going to  $\alpha$  cerium,  $\Delta V/V \approx 17\%$ <sup>[3]</sup>.) An explanation was proposed back in 1949-1950 by Zachariasen<sup>[4]</sup> and Pauling<sup>[5]</sup>. It is based on the fact that the 4f levels of rare-earth atoms, particularly cerium, lie high in energy, near the levels of the outer valence 6s(p) and 5d electrons. At the same time, the radial wave function of the 4f electron has a maximum in the region of the 4s(p)d shells, i.e., the 4f electron lies in the interior of the atom in the radial direction (the average radius of its "orbit" is several times smaller than the atomic radius determined by the outer valence electrons). When pressure is applied (hydrostatic compression of the atom), the 4f level may be "crowded out" of the potential well and the transition 4f  $\rightarrow$  valence (e.g., 5d) level can turn out to be more favored energywise. The crowding out of the 4f electron is accompanied by a sharp compression of the higher-lying electronic shells, owing to the increase in the effective Coulomb potential in which they are situated, i.e., by a decrease of the atomic radius and accordingly of the crystal-lattice parameter (5.16 Å for  $Ce_{\gamma}$  and 4.85 Å for  $Ce_{\alpha}$  in a transition under pressure at room temperature). The electronic configurations are usually taken in the form  $4f^x 5d^{2-x} 6s^2$ , where  $x \approx 1$  (0.9)<sup>[3]</sup> for  $Ce_{\gamma}$  and  $x \approx 0.5$  (0.4)<sup>[3]</sup> for  $Ce_{\alpha}$ : Nearly trivalent  $\gamma$  cerium goes over into  $\alpha$  cerium, which is closer to tetravalent. When the pressure is removed, the inverse process takes place, namely "collapse" of one of the electrons of the sd conduction band into the 4f state.

This lucid model seemed to correspond to the available experimental data (see, e.g.,<sup>[3]</sup>) and served as a basis for detailed theoretical studies both of the atomic "pushing out" process (within the framework of Hartree-Fock calculations with a movable Wigner-Seitz boundary<sup>[6]</sup>), and of the accompanying changes in the properties of cerium metal (within the framework of the

band theory, which assumes the 4f-5d transition as the initial fact<sup>[7, 8]</sup>). At the same time, there was no experimental confirmation of the proposed electronic mechanism. Moreover, in 1964-1972, studies of two-quantum annihilation of positrons<sup>[9-11]</sup> yielded results that did not confirm the foregoing picture. The expected decrease in the positron lifetime (following an increase in the number of valence electrons after the  $Ce_{\gamma}$ - $Ce_{\alpha}$  transition) and the broadening of the angular distribution of the  $\gamma$  quanta were found in the experiment to be either small in comparison with the calculated values<sup>[12]</sup> (in the case when the transition is initiated by pressure), or even of opposite sign (in the low-temperature transition). The authors of these papers reached the conclusion that their data refute the hypothesis of the 4f-5d crowding-out and agree with the model of the so-called spin compensation<sup>[13]</sup>. These results were used in an attempt to review the overall explanation of the pT diagram of cerium<sup>[14]</sup>.

The idea of our paper consists of using (to answer the question as to whether the number of collapsed 4f electrons of  $\gamma$  cerium is altered in the  $Ce_{\gamma}$ - $Ce_{\alpha}$  transition, and to what degree) the effect of the so-called chemical shift of the x-ray lines<sup>[15, 16]</sup>. The effect consists of a small but measurable change in the energy of the principal x-ray lines of the K series when restructuring takes place in the outer valence shells (change in the orbital quantum number  $l$  or "drawing away" of the valence electrons when an ionic chemical bond is produced). The magnitudes and signs of the shifts and also the shapes of the plots of the displacement against the type of line ( $K_{\alpha 1}$ ,  $K_{\beta 1}$ ,  $K_{\beta 2, 4}$ ) are different when electrons of different  $l$ -type (s, p, d, or f electrons) are involved in the chemical bond or are removed. These plots turned out to be particularly characteristic for the 4f electrons of rare-earth (RE) elements, this being due, briefly speaking (details can be found in<sup>[16]</sup>), to the anomalously deep radial location of the 4f electron and consequently to the anomalously strong perturbation of the remaining shells of the atom when this electron is removed or goes over to 5d, 6s(p) levels.

Figure 1 (dashed and dash-dot lines) shows the experimental plots of the displacement against the type of line for the compound pairs  $EuF_2$ - $EuF_3$  and  $SmCl_2$ -

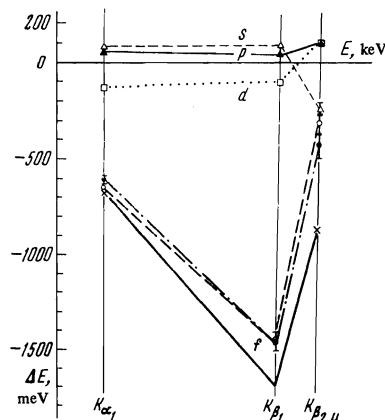


FIG. 1. Effect of chemical shift of the principal K-series x-ray lines if one of the 4f electrons is removed. Plots: effect vs. type of line [16]. Dashed and dash-dot curves - experiment for  $\text{EuF}_2\text{-EuF}_3$  and  $\text{SmCl}_2\text{-SmF}_3$ , respectively. Solid curve - Hartree-Fock-Slater calculation (relativistic) for Eu ions (configurations  $4f^7 - 4f^6$ , boundary conditions at infinity, Hartree-Fock-Slater-Latter,  $C = 1$ ). At the top are shown analogous plots for 6s(p) or 5d electrons.

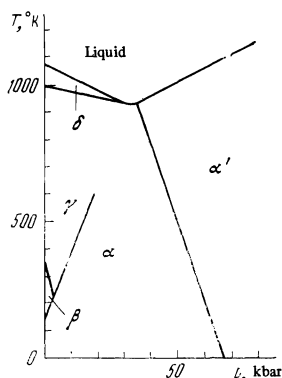


FIG. 2. Phase diagram of Ce [14]. Phases  $\gamma$ ,  $\alpha$ , and  $\alpha'$  are face-centered cubic, phase  $\beta$  is hexagonal close-packed, and phase  $\delta$  is body-centered cubic.

$\text{SmF}_3$ . [16] In these compounds, with practically 100% ionicity of the bonds, the RE ions have configurations  $4f^7 - 4f^6$  in the case of europium and  $4f^6 - 4f^5$  in the case of samarium, the difference within each pair amounting to one 4f electron. A theoretical curve is also shown for  $\text{Eu}^{2+} - \text{Eu}^{3+}$ , calculated (see [16,17]) within the framework of the Hartree-Fock-Slater (HFS) method and offering evidence of a perfectly satisfactory understanding of the nature of this dependence. In the upper part of the figure are shown analogous plots for 6s(p) and 5d electrons, which make it possible to compare the character and the scales of the effects.

One could hope thus that if the phase transition in cerium is indeed connected with a removal of a 4f electron (transition to the 5d, 6s(p) state), then a comparison of the  $K_{\alpha_1}$ ,  $K_{\beta_1}$ , and  $K_{\beta_{2,4}}$  lines of  $\gamma$  and  $\alpha$  cerium should reveal large shifts, resulting in a characteristic V-shaped plot analogous to the curves of Fig. 1, something difficult to obtain as a result of any other electronic restructuring.

### EXPERIMENTAL INVESTIGATION OF THE $\gamma$ - $\alpha$ TRANSITION INITIATED IN CERIU BY HIGH EFFECTIVE PRESSURE IN LAVES PHASES

Figure 2 shows the phase diagram of cerium (see, e.g., [14]). There are obviously two methods of obtaining the  $\gamma$ - $\alpha$  transition: low-temperature (at normal pres-

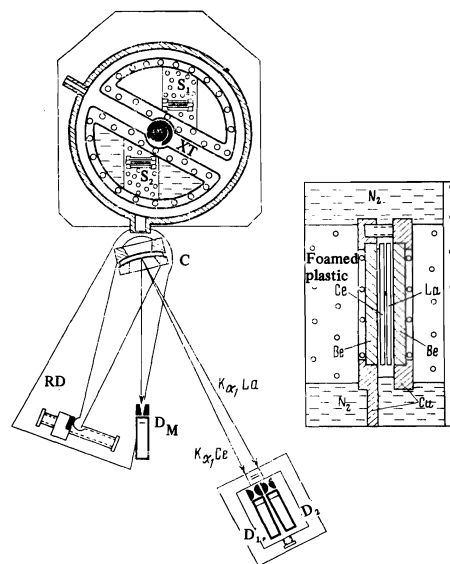


FIG. 3. Experimental setup for the low-temperature experiment. Right - arrangement of the source when working as a dilatometer. The lanthanum disk was removed before the start of low-temperature measurements of the shifts.

sure) and by application of pressure (at normal temperature).

The low-temperature  $\gamma$ - $\alpha$  transition was initiated in our case by cooling  $\text{Ce}_\gamma$  with liquid nitrogen ( $T = 77^\circ\text{K}$ ) or helium ( $T = 4.2^\circ\text{K}$ ). The experiments included both measurement of small energy shifts of the x-ray  $K_{\alpha_1}$ ,  $K_{\beta_1}$ , and  $K_{\beta_{2,4}}$  lines and measurement of the concentration of the produced  $\alpha$  phase (knowledge of the latter is essential for the calculation of the shift corresponding to a complete (100%)  $\gamma$ - $\alpha$  transition). The shifts were measured by a method previously developed for the study of chemical and isotopic shifts of x-ray lines [16,20] (the method is based on alternately introducing the compared objects into the field of view of a special Cauchois-type crystal-diffraction spectrometer).

The experimental setup is shown in Fig. 3. The fluorescent radiation in samples  $S_1$  or  $S_2$ , which were alternately introduced into the field of view of the instrument, was excited by an x-ray tube XT (we used an RUP-150 commercial x-ray apparatus,  $I = 10$  mA,  $U = 150$  kV) and was extracted through a cylindrical collimator ( $\phi$  12 mm) to a bent quartz crystal C (reflecting planes 1340, thickness 1 mm, radius of bend 2 m, flexure coefficient of the reflecting planes  $k = 2 \times 10^{-4} \text{ cm}^{-1}$  [18]). The crystal was rotated with the aid of a precision reading device RD, analogous to the reading device described in [19]. The diffracted radiation passing through a receiving slit placed on the focal circle (width  $200 \mu$ ) was registered with a scintillation detector  $D_1$ .

The compared samples of rolled and annealed metallic cerium (purity  $\geq 99.9\%$ ) in the form of disks of 20 mm diameter and optimal thickness  $\approx 200 \mu$  [20] were fastened on copper cold fingers in identical foamed-plastic Dewars (Fig. 3, right). To prevent possible bending by cooling, the sample was clamped between two beryllium washers.

To improve the stability, we used a monitoring system. The scintillation monitor detector,  $D_M$ , was placed in the direct fluorescent beam from the investigated

sample. The time required to accumulate the statistics in the counting channel was determined by the time required to accumulate the specified number of counts in the monitoring channel.

When the apparatus was constructed, it was found difficult to provide for sample rotation to compensate for aperture aberration<sup>[20]</sup>, but the possible aberration shifts were eliminated by constructing the main units of the spectrometer with increased accuracy. In particular, an increase in the dimensions of the bending steel mirrors and of the crystal (65×70 mm, window 35×35 mm) has made it possible to work with 1/10 of the area of the total aperture at sufficient intensities. (The counting rate at the maximum of the  $K_{\alpha 1}$  line of Ce was 25000  $\text{min}^{-1}$  at a background of 150  $\text{min}^{-1}$ .) The maximum value of the aperture aberration within the limits of the total (35×35 mm) aperture, determined as the shift (on the focal circle) of the  $K_{\alpha 1}$  line after passage of the radiation through individual small (6 mm diameter) sections of the crystal did not exceed 10  $\mu$  in this case. The receiving slits of the spectrometer detectors were made up of glass semicylinders finished with optical accuracy (the deviation from parallelism of the cylinder generatrices was  $\approx 1 \mu$ ).

To check the operation of the instrument as a whole, we measured the shifts of the  $K_{\alpha 1}$ ,  $K_{\beta 1}$ , and  $K_{\beta 2,4}$  lines of  $\text{CeO}_2$  and of metallic Ce. Within the limits of the measurement errors, the shifts agreed with the results obtained with the setup with rotating specimens (see Table IV below). The degree of absence of aberration can also be assessed from the results of "null" experiments carried out before or after each low-temperature experiment and consisting of measurement of the shifts for the same samples, but at identical temperatures—either both at room temperature or both at nitrogen temperature. The average values of the shift and the rms errors for the null experiments are listed in Table I (lines 3 and 4).

The amount of  $\text{Ce}_\alpha$  produced from  $\text{Ce}_\gamma$  upon cooling was monitored and measured with the aid of a "lanthanum dilatometer." A sample of metallic La (Fig. 3, right) was placed in front of the Ce sample. Over the receiving slit used to register the Ce radiation we placed a second identical receiving slit with a scintillation detector ( $D_2$  in Fig. 3) to register La radiation. The position of the slit  $D_2$  on the focal circle is chosen such that when the principal channel  $D_1$  was tuned to the maximum of the  $K_{\alpha 1}$  line of Ce, the auxiliary slit was at the  $K_{\alpha 1}$  maximum of La. With such a geometry, the intensity of the  $K_{\alpha 1}$  La line passing through the cerium foil depends on the density of the cerium and the density change due to the change in the phase composition upon cooling can be measured from the change in the intensity ratio of the  $K_{\alpha 1}$  lines of La and Ce.

TABLE I. Control measurements in the low-temperature  $\text{Ce}_\gamma - \text{Ce}_\alpha$  Experiment

No.	$\nu_N/\nu_R$	$\Delta E_{K_{\alpha 1}}$ , meV	$\Delta E_{K_{\beta 1}}$ , meV	$\Delta E_{K_{\beta 2,4}}$ , meV	Note
1	—	$-20 \pm 6$	$-39 \pm 11$	—	$\text{Ce}_\beta - \text{Ce}_\gamma$ Both samples at room temperature
2	$4.001 \pm 0.002$	$-49 \pm 8$	$-49 \pm 14$	$1 \pm 45$	$\text{Ce}_\beta - \text{Ce}_\gamma$ $t_\beta = 77^\circ \text{K}$ , $t_\gamma = \text{room}$
3	—	$0 \pm 3$	$8 \pm 7$	—	$\text{Ce}_\gamma - \text{Ce}_\gamma$ Both samples at nitrogen temperature
4	—	$1 \pm 4$	—	—	$\text{Ce}_\alpha - \text{Ce}_\alpha$ Both samples at nitrogen temperature

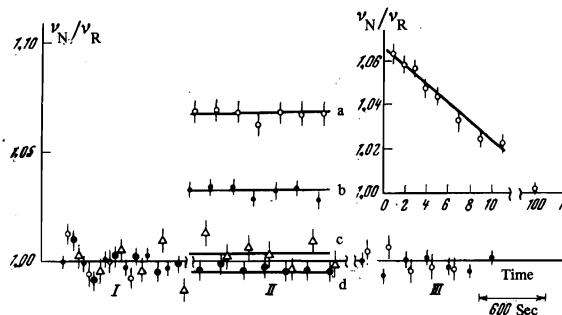


FIG. 4. Readings of lanthanum dilatometer: I - room temperature, II - liquid-nitrogen temperature, III - room temperature; a - abrupt cooling in liquid nitrogen, compression in nitrogen to  $p \approx 3000 \text{ kg/cm}^2$ , removal of pressure; b - abrupt quenching in nitrogen, c - after 100 cycles consisting of heating to room temperature and cooling in nitrogen; d - control experiment with lanthanum placed behind the cerium. Upper right - dependence on the number of the thermal cycles.

It is easy to obtain for the concentration of the  $\alpha$  cerium produced in the sample the expression

$$C_\alpha = \frac{\Delta\rho_{\gamma-\alpha}}{\rho_\alpha - \rho_\gamma} \approx \frac{3}{2} \left( \frac{\rho_\alpha}{\rho_\alpha - \rho_\gamma} \right) \left\{ \frac{1}{\mu_\gamma \rho_\gamma} \ln \frac{\nu_N}{\nu_R} - \frac{1}{\mu_\beta \rho_\beta} \ln \frac{\nu'_N}{\nu'_R} \right\}. \quad (1)$$

Here  $\Delta\rho_{\gamma-\alpha}$  is the change in the sample density as measured by the lanthanum dilatometer in the case of a partial  $\gamma - \alpha$  transition,  $\rho_\alpha$  and  $\rho_\gamma$  are the densities of the  $\alpha$  and  $\gamma$  cerium,  $\mu_\gamma$  and  $\mu_\beta$  are the coefficients for the absorption of the lanthanum  $K_{\alpha 1}$  radiation in  $\gamma$  and  $\beta$  cerium, determined in the experiment directly on the investigated samples,  $\nu_N \equiv (N\text{Ce}_e/N\text{La})t_N$  and  $\nu_R \equiv (N\text{Ce}_e/N\text{La})t_R$  are the ratios of the counts at the maxima of the  $K_{\alpha 1}$  lines of cerium and lanthanum at the temperature of liquid nitrogen ( $t_N$ ) and at room temperature ( $t_R$ ). The second term in the curly brackets indicates the normal temperature compression of the sample, not connected with the  $\text{Ce}_\gamma - \text{Ce}_\alpha$  transition. It was determined experimentally with samples in which  $\beta$  cerium, which hinders the  $\gamma - \alpha$  transition, was accumulated as a result of repeated thermal cycling ( $\approx 100$  cycles) between room and nitrogen temperatures<sup>[21]</sup>. (It was assumed that the average coefficients of temperature compression of  $\gamma$ ,  $\beta$ , and  $\alpha$  cerium were the same in the employed temperature range.)

Figure 4 shows the experimental ratios of the counts of the  $K_{\alpha 1}$  lines of Ce and La, normalized to the average value of  $\nu_R$  in region I, as functions of the temperature and the prior history of the samples. The decrease of the ratio  $\nu_N/\nu_R$  with increasing number of cycles on the upper-right plot corresponds to the loss of the  $\alpha$  phase with increasing accumulation of the  $\beta$  phase. The influence of the methods used by us to convert  $\text{Ce}_\gamma$  into  $\text{Ce}_\alpha$  (see, e.g.,<sup>[21,22]</sup>) on the concentration of the Ce measured with the lanthanum dilatometer can be seen from Table II. The measurements were performed either before or after the experimental determination of the line shifts (in the former case,  $\nu_R$  was measured before cooling the sample, and in the latter after heating the sample). Control measurements of the accumulation of the  $\alpha$  phase after keeping the sample for 100 hours in nitrogen revealed no additional change (within the limits of the experimental error) in the phase composition.

The presence of the  $\beta$  phase on top of the  $\alpha$  phase in a sample cooled only once called for additional control

measurements of the shifts due to the  $\beta$  phase. The energy difference of the x-ray lines from the cooled ( $C_{e\alpha,\beta,\gamma}$ ) and uncooled ( $C_{e\gamma}$ ) samples can be expressed in the form

$$\Delta E = C_\alpha \Delta E_\alpha + C_\beta \Delta E_\beta, \quad (2)$$

where  $\Delta E$  is the experimentally measured energy difference,  $\Delta E_\alpha$  is the difference between the energies of the lines of  $\alpha$  and  $\gamma$  cerium,  $\Delta E_\beta$  is the difference between the energies of the lines of  $\beta$  and  $\gamma$  cerium, and  $C_\alpha$  and  $C_\beta$  are the concentrations of the  $\alpha$  and  $\beta$  phases. The quantity  $\Delta E_\beta$  was determined in experiments with samples that had gone through 100 thermal cycles. In this case,  $C_\alpha \approx 0$  and  $C_\beta \approx 0.8$  [21]. The values of the shift  $\Delta E_\beta$  are given in Table I; the measurements were performed with the  $\beta$  samples both at nitrogen and at room temperature; within the limits of the experimental errors, the line shifts are in agreement. This, like the dilatometric data  $\nu'_N/\nu'_R = 1.001 \pm 0.002$ , indicates that there is no  $\alpha$  transition when samples with  $C_{e\beta}$  are cooled to nitrogen temperature.

The experimental shifts  $\Delta E$  of the lines  $K_{\alpha 1}$ ,  $K_{\beta 1}$  and  $K_{\beta 2,4}$  from low-temperature  $C_{e\alpha}$ -containing samples and the corresponding values of the  $\alpha$ -phase concentration  $C_\alpha$ , measured with the dilatometer, are compared

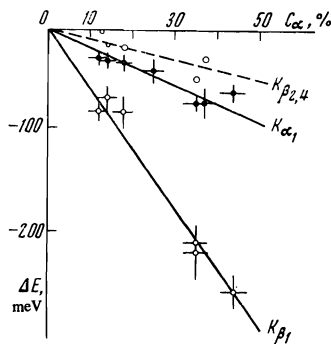


FIG. 5. Dependence of the experimental values of the shifts of the  $K_{\alpha 1}$ ,  $K_{\beta 1}$ , and  $K_{\beta 2,4}$  lines ( $\Delta E$ ) on the concentrations ( $C_\alpha$ ) of the  $\alpha$  phase in the sample.

in Table II. We see that the correction for  $C_{e\beta}$  is essential, since the concentration of the  $\beta$  phase in the case of abrupt single quenching is on the order of 20% [21,23], and the quantity  $C_\beta \Delta E_\beta$  is small and within one standard deviation from  $\Delta E$ . Plots of the experimentally measured K-line shifts against the  $C_{e\alpha}$  concentration are also shown in Fig. 5. The straight lines were drawn by least squares<sup>1)</sup>. The shift  $\Delta E_0$  (Table II), corresponding to a 100% conversion of  $\gamma$  cerium into  $\alpha$  cerium, was calculated in the form  $\Delta E_0 = \Delta E/C_\alpha$ . The weighted average shifts  $\Delta E_0$  obtained from eight experiments for the corresponding lines are shown at the bottom of Table II. The errors are mean-squared. The values of  $\Delta E_0$  are shown in Fig. 6 as functions of the energy of the corresponding line (solid straight line). The same figure shows the results of the control experiment, namely the differences between the energies of the K lines of  $\beta$  and  $\gamma$  cerium ( $\beta$  cerium at nitrogen temperature, dashed straight line), and the results of a "null" experiment, namely the shift of the  $K_{\alpha 1}$  and  $K_{\beta 1}$  lines of identical samples:  $C_{e\gamma} - C_{e\gamma}$ .

### EXPERIMENTAL INVESTIGATION OF $\gamma$ - $\alpha$ TRANSITION IN METALLIC CERMIUM AT LOW TEMPERATURE

In addition to the low-temperature  $C_{e\gamma} - C_{e\alpha}$  transition described above, we have attempted to initiate the same transition with pressure, by placing the Ce atoms in a lattice of intermetallic compounds, the so-called Laves phases (general formula  $RX_2$ , structure type C15, see, e.g., [24]). The main factor influencing the formation of these phases is the space-geometry requirement that the ratio  $d_R/d_X$ , where  $d_R$  and  $d_X$  are respectively the distances between the atoms R or X in the Laves phase, should be  $1.225 \equiv K_0$ . Since the ratio of the corresponding quantities (atomic diameters) in the lattices of the pure components  $D_R/D_X \equiv K$  deviates from this ideal value, the R and X atoms in the Laves phase expand or contract [24]. We have chosen for the investigation Laves phases in which the R element is Ce, and the value of K is either close to  $K_0$ , so that the atom Ce experiences no significant compression (tension), or else K is much

TABLE II. Results of low-temperature  $C_{e\gamma} - C_{e\alpha}$  Experiment

$C_\alpha$	$K_{\alpha 1}$		$K_{\beta 1}$		$K_{\beta 2,4}$		Method of initiating the $\gamma$ - $\alpha$ transition
	$\Delta E$ , meV	$\Delta E/C_\alpha$ , meV	$\Delta E$ , meV	$\Delta E/C_\alpha$ , meV	$\Delta E$ , meV	$\Delta E/C_\alpha$ , meV	
$0.12 \pm 0.02$	$-29 \pm 4$	$-242 \pm 52$	$-80 \pm 9$	$-667 \pm 134$	$-3 \pm 24$	$-25 \pm 200$	Abrupt (4000° K/min) cooling with nitrogen
$0.14 \pm 0.02$	$-31 \pm 4$	$-221 \pm 42$	$-67 \pm 11$	$-478 \pm 104$	$-17 \pm 31$	$-121 \pm 221$	Ditto
$0.18 \pm 0.02$	$-33 \pm 6$	$-183 \pm 39$	$-81 \pm 15$	$-450 \pm 97$	$-19 \pm 31$	$-106 \pm 173$	"
$0.25 \pm 0.02$	$-40 \pm 9$	$-160 \pm 38$	—	—	—	—	Abrupt cooling with helium followed by placement in nitrogen
$0.35 \pm 0.03$	$-72 \pm 7$	$-206 \pm 27$	$-206 \pm 16$	$-588 \pm 68$	—	—	Abrupt cooling with nitrogen; compression in nitrogen (P $\approx 3000$ kg/cm <sup>2</sup> ), removal of pressure, storage in nitrogen
$0.35 \pm 0.03$	—	—	$-216 \pm 23$	$-617 \pm 84$	$-49 \pm 43$	$-140 \pm 123$	Ditto
$0.37 \pm 0.03$	$-71 \pm 14$	$-192 \pm 41$	—	—	$-30 \pm 56$	$-81 \pm 151$	"
$0.44 \pm 0.03$	$-61 \pm 7$	$-139 \pm 18$	$-253 \pm 16$	$-575 \pm 53$	—	—	"
Average	$-173 \pm 14$ external		$-566 \pm 26$ external		$-103 \pm 19$ external		
$\Delta E_0 \equiv \Delta E/C_\alpha$	$-173 \pm 12$ internal		$-566 \pm 32$ internal		$-103 \pm 73$ internal		

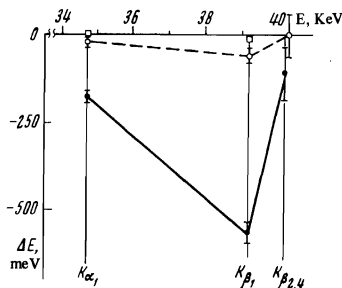


FIG. 6. Experimental plots of the shift against type of line in low-temperature  $Ce_{\gamma} - Ce_{\alpha}$  transition. Dashed - control experiment with sample "poisoned" with  $\beta$  cerium ( $C_{\beta} \approx 80\%$ , shift normalized to 100%  $C_{\beta}$  content). The rectangles at the top denote the null experiment with both samples at the same temperature

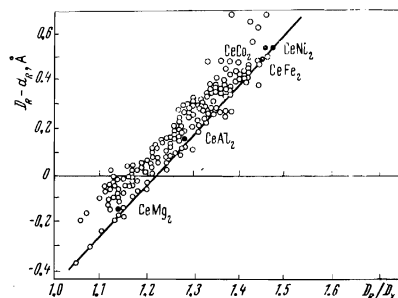


FIG. 7. Changes in the interatomic distances between the R components on going from the pure-metal lattice ( $D_R$ ) to the Laves phase ( $d_R$ ), as functions of the ratio of the atomic radii of the pure R and X components for most known Laves phases [24]. The dark circles show the positions of the Laves phases investigated by us.

larger than  $K_0$  and the Ce atom is compressed (see the first two columns of Table III). The pressures  $p$  experienced by the cerium atoms can easily be estimated if one knows the change in the atomic diameter of the Ce in the Laves phase in comparison with pure  $Ce_{\gamma}$ . Ascribing this change to the influence of the hydrostatic compression, we can write  $\Delta V/V = \chi p$ , where  $\chi$  is the coefficient of hydrostatic compression of Ce. Such estimates give for the  $CeNi_2$ ,  $CeFe_2$ , and  $CeCo_2$  phases pressures on the order of 100 kbar, i.e., perfectly sufficient to initiate  $\gamma - \alpha$ , and perhaps also  $\gamma - \alpha'$  transitions in Ce (see Fig. 2). A similar conclusion is also reached by simple comparison of the interatomic (Ce-Ce) distances  $D_R$  in  $\gamma$ ,  $\alpha$ , and  $\alpha'$  cerium, which are respectively 3.648, 3.430, and 3.296 Å [25], with the same quantities for the chosen Laves phases, which are given in the third column of Table III.

If the different modifications of Ce actually differ in the number of 4f electrons, then we should expect the appearance of characteristic shifts (of the type shown in Fig. 1) of the  $K_{\alpha 1}$ ,  $K_{\beta 1}$ , and  $K_{\beta 2,4}$  lines of cerium in  $CeFe_2$ ,  $CeCo_2$ , and  $CeNi_2$  in comparison with  $Ce_{\gamma}$ . Experiments with  $CeMg_2$  and probably also  $CeAl_2$  could serve as the null experiments.

Removal of a 4f electron from a Ce atom can be initiated, however, not only by pressure and temperature, but also by chemical-interaction forces. We have therefore attempted to choose Laves phases in which the chemical interaction between the R and X atoms is minimal, using the following selection criterion [26]. Figure 7 shows the changes of the atomic diameters of the component R in the Laves phase in comparison with the pure metal as functions of the quantity  $K \equiv D_R/D_X$  for most known Laves phases. The points on this diagram are grouped into a strip with a distinctly outlined lower edge. It is important that the line drawn through the points of the lower edge intersects the zero-compression line at  $K = K_0 \equiv 1.225$ . Obviously, the minimal compression necessary to satisfy the space and geometry requirements is realized for the Laves phases lying along this line. For the remaining Laves phases, there exists an additional compression, which is usually attributed to the presence of chemical interaction between the R and X atoms. As seen from Fig. 7, the Laves phases chosen by us lie near the straight line.

The Laves phases were prepared by arc melting in an argon atmosphere. The purities of the initial metals were 99.0% for Ce, and 99.99, 99.9, 99.9, 99.83, and 99.98% for Al, Mg, Fe, Ni, and Co, respectively. The

TABLE III. Experimental shifts of K-series x-ray lines of cerium in Laves phases relative to  $Ce_{\gamma met}$

Investigated compound	$K = \frac{D_R}{D_X}$	$d_R, \text{Å}$	$\Delta E \equiv E_{CeX_n} - E_{Ce_{\gamma}}, \text{meV}$			$\eta$ , fractions of 4f-5d transition
			$K_{\alpha 1}$	$K_{\beta 1}$	$K_{\beta 2,4}$	
$CeMg_2$	1.139	3.777	$-17 \pm 9$	$-6 \pm 16$	$+16 \pm 29$	$0.01 \pm 0.01$
$CeAl_2$	1.274	3.491	$-7 \pm 13$	$-6 \pm 24$	$+11 \pm 46$	$0.01 \pm 0.01$
$CeFe_2$	1.433	3.161	$-126 \pm 10$	$-407 \pm 20$	$-118 \pm 36$	$0.36 \pm 0.02$
$CeCo_2$	1.458	3.100	$-138 \pm 11$	$-480 \pm 30$	$-115 \pm 50$	$0.43 \pm 0.02$
$CeNi_2$	1.464	3.128	$-79 \pm 10$	$-304 \pm 20$	$-70 \pm 40$	$0.26 \pm 0.02$

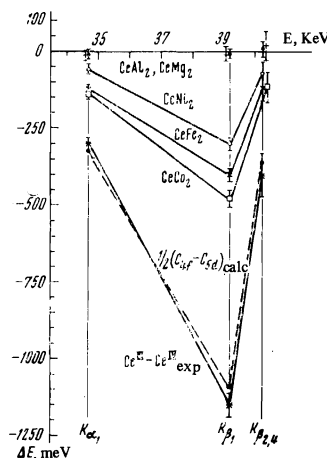


FIG. 8. Experimental plots of the shift against the line type for the  $Ce_{\gamma} - Ce_{\alpha}$  transition in Laves phases. The figure (lower curves) shows also the experimental and theoretical (dashed) plots on going from trivalent ( $Ce^{III}$ ) to tetravalent ( $Ce^{IV}$ ) cerium. The calculated values of  $C_{4f} - C_{5d}$  were divided by two.

agreement between the obtained structures and the required ones was verified by plotting the Debyeograms.

The measurements were performed with an installation previously used to investigate chemical shifts, using the standard procedure (see, e.g., [16,20]). The experimental values of the shifts of the investigated lines are shown in the 4th, 5th, and 6th columns of Table III and in Fig. 8. As seen from Table III and Fig. 8, the shifts of the  $CeFe_2$ ,  $CeCo_2$ , and  $CeNi_2$  Laves phases have negative signs on all lines and the characteristic V-shaped dependence of the shift on the type of the investigated line, thus offering unambiguous evidence of partial removal of a 4f electron from the Ce atom. In  $CeMg_2$  and  $CeAl_2$ , no removal of a 4f electron from the Ce atom takes place (the shifts are close to zero on all lines).

TABLE IV. Experimental shifts of K-series x-ray lines of cerium between different trivalent and tetravalent compounds of cerium (in meV).

Compared compounds	$K_{\alpha_1}$	$K_{\beta_1}$	$K_{\beta_{3,4}}$
CeF <sub>3</sub> — Ce <sub>γ</sub> met	-22 ± 15	—	—
CeCl <sub>3</sub> — Ce <sub>2</sub> (C <sub>2</sub> O <sub>4</sub> ) <sub>3</sub>	+7 ± 20	—	—
CeO <sub>2</sub> — Ce <sub>γ</sub> met	-433 ± 9	-1126 ± 17	-349 ± 18
	-422 ± 14 *	-1091 ± 40 *	-360 ± 50 *
CeO <sub>2</sub> — CeF <sub>3</sub>	-410 ± 10	-1240 ± 25	-288 ± 36
CeO <sub>2</sub> — CeCl <sub>3</sub>	-390 ± 20	—	—
CeO <sub>2</sub> — Ce <sub>2</sub> (C <sub>2</sub> O <sub>4</sub> ) <sub>3</sub>	-385 ± 20	—	—
(NH <sub>4</sub> ) <sub>2</sub> Ce(NO <sub>3</sub> ) <sub>6</sub> — Ce <sub>2</sub> (C <sub>2</sub> O <sub>4</sub> ) <sub>3</sub>	-416 ± 10	—	—
C <sub>4f</sub>	-410 ± 20	-1200 ± 40	-400 ± 120
C <sub>5d</sub>	-300 ± 20	-1150 ± 40	-390 ± 120

\*The results were obtained with the installation used for the low-temperature experiment without rotating the samples.

From the experimental shifts we can calculate the fraction  $\eta$  of the 4f electrons removed from the Ce atoms in the investigated Laves phases, if we know the shifts following complete removal of one 4f electron from a Ce atom. The latter were measured by us experimentally in trivalent and tetravalent cerium compounds.

The shifts for different trivalent-trivalent Ce compound pairs and tetravalent-tetravalent Ce compound pairs are shown in Table IV. It is important that the shifts for different compounds of trivalent and tetravalent cerium coincide within the limits of experimental errors. This indicates that the valence obtained in the investigated chemical compounds of Ce is either III or IV, and that there are no intermediate fractional valences, since it is little likely that this intermediate valence would be the same for all the investigated chemical compounds. There are therefore grounds for assuming that the experimental shifts between tetravalent and trivalent compounds correspond to complete removal of one 4f electron from the Ce atom.

In the calculation of the values of  $\eta$  we have also assumed that the 4f electron of Ce goes off to the 5d band<sup>2)</sup>. Under this assumption, the shift of the Ce x-ray lines in the Laves phases, relative to Ce<sub>γ</sub>met, takes the form

$$\Delta E_{\text{CeX}_2-\text{Ce}_\gamma} = \eta(C_{4f} - C_{5d}), \quad (3)$$

where  $C_{4f}$  and  $C_{5d}$  are coefficients equal to the shifts of the investigated lines following complete removal of 4f and 5d electrons from the Ce atom, respectively. The values of  $C_{4f}$  were determined from the experimental shifts between the tetravalent and trivalent compounds of Ce by introducing corrections for the contribution made by other valence electrons (with the exception of 4f), in analogy with the procedure used for example, in [27]. The values of  $C_{5d}$  were calculated theoretically within the framework of the HFS method (see [16] and below). Table IV lists the mean values of  $C_{4f}$  and  $C_{5d}$ , calculated from all the experimental shifts between the tetravalent and trivalent compounds of Ce. The errors are assumed to be equal to the maximum deviation from the mean. The obtained values of  $C_{4f}$ - $C_{5d}$  as functions of the type (energy) of the line are also shown in Fig. 8 (the curve Ce<sup>III</sup>-Ce<sup>IV</sup><sub>exp</sub>). Relation (3) was used to obtain the values of  $\eta$  for all the investigated Laves phases. These quantities are given in the last column of Table III and constitute the weighted average values of  $\eta$ , determined for each of the investigated  $K_{\alpha_1}$ ,  $K_{\beta_1}$ , and  $K_{\beta_{3,4}}$  lines.

## CALCULATIONS WITHIN THE FRAMEWORK OF THE HARTREE-FOCK-SLATER METHOD WITH WIGNER-SEITZ BOUNDARY CONDITIONS

The experimental data (Fig. 6 and 8) offer sufficiently unequivocal evidence concerning the mechanism of the investigated effect. Nonetheless, it is of interest to attempt to compare these experimental data with theoretical ones. Such an opportunity is afforded by calculations within the framework of the self-consistent models of the Hartree-Fock type, when the line shifts can be expressed in terms of the eigenvalues  $\epsilon$  of the corresponding levels, calculated for specified valence configurations of the atoms or ions. For example, for the configurations A(4f<sup>0.5</sup>5d<sup>1.5</sup>6s<sup>2</sup>) and B(4f<sup>1</sup>5d<sup>1</sup>6s<sup>2</sup>) we have

$$\Delta E_{K_{\alpha_1}} = (\epsilon_{1s\gamma_A} - \epsilon_{2p_{3/2}})_A - (\epsilon_{1s\gamma_B} - \epsilon_{2p_{3/2}})_B. \quad (4)$$

Comparison of similar calculations, performed for free atoms (boundary conditions as  $r \rightarrow \infty$ ) with experiment have, in general, shown satisfactory agreement [16]. The results of such calculations for europium are shown and compared with experiment in Fig. 1. The dashed lines in Fig. 8 show the results of the calculation made in the present paper for configurations A and B of cerium. A striking similarity is observed between the experimental curve (Ce<sup>III</sup>-Ce<sup>IV</sup><sub>exp</sub>) corresponding to C<sub>4f</sub>-C<sub>5d</sub> and the calculated curve. The latter, however, obviously corresponds to (C<sub>4f</sub>-C<sub>5d</sub>)/2, i.e., in fact the calculated values are approximately double the experimental ones.

The values of the shifts and the character of the plots of the shift against the line types, due to 4f electrons, turn out to depend relatively little (the change  $\Delta E$  does not exceed  $\approx 30\%$ ) on the following detailed assumptions made in the calculation: different ways of taking into account the exchange interaction ( $C=1$  or  $C=2/3$  in the expression for the exchange potential after Slater [28]), allowance (HFSL) or no allowance (HFS) for the Latter correction [29], which takes into account the asymptotic form of the potential  $U(r)$ .

In the case of the Ce<sub>γ</sub>-Ce<sub>α</sub> transformation of interest to us, this model should be modified [6] by a transition to the boundary conditions on the Wigner-Seitz (WS) sphere with radius  $R_{WS}$ , a sphere imitating the coordination polyhedron in the crystal. The boundary conditions on the WS sphere were taken by us in the form [30]

$$\left. \frac{dg}{dr} \right|_{r=R_{WS}} = 0 \quad \text{for } l \text{ even,} \\ g(r) \Big|_{r=R_{WS}} = 0 \quad \text{for } l \text{ odd,} \quad (5)$$

where  $g$  is the larger WS component of the radial Dirac wave function.

Figure 9 shows plots of the total energy of the atom

$$E_x = - \sum_i \left[ \epsilon_i + \frac{1}{2} \int_0^{R_{WS}} (g_i^2 + f_i^2) (\alpha Z r + U(r)r^2) dr \right] \quad (6)$$

against the volume  $V_{WS}$  of the WS sphere for different electronic configurations of the cerium atom (here  $f$  is the smaller component of the radial Dirac wave function). Obviously, calculations of this type should be referred to absolute zero temperature. The position of the minimum of each curve determines the equilibrium volume (at zero pressure  $p = -dE_x/dV = 0$ ) of the WS sphere (the volume of the atom). The absolute minimum of the total energy is reached for the configurations 4f<sup>0.4-0.5</sup>5d<sup>1.5-1.6</sup>6s<sup>2</sup>, which are usually ascribed to  $\alpha$

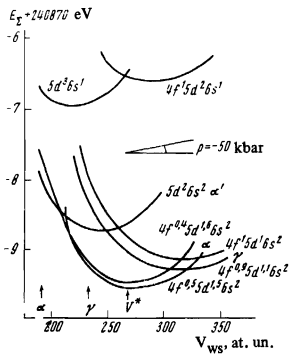


FIG. 9

FIG. 9. Calculated plots of the total energy against the volume of the WS sphere for different electronic configurations of the cerium atom. The symbols  $\gamma$ ,  $\alpha$ , and  $\alpha'$  denote curves ascribed to  $\gamma$ ,  $\alpha$  and  $\alpha'$  cerium; the arrows with indices  $\gamma$  and  $\alpha$  show the experimental volumes of the WS spheres. In the center is shown the slope angle corresponding to a pressure 50 kbar.

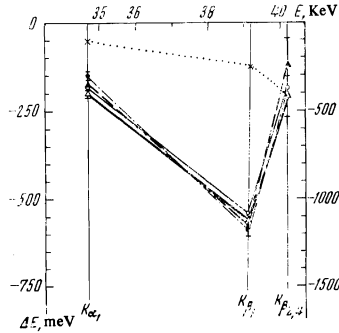


FIG. 10

FIG. 10. Experimental and normalized theoretical plots for  $\text{Ce}^{\text{III}} - \text{Ce}^{\text{IV}}$  (experiment - dash-dot lines, calculation - thin solid line, right-hand ordinate scale), and  $\text{Ce}_\gamma - \text{Ce}_\alpha$  (low-temperature experiment - dashed, calculation - thick solid line, left-hand ordinate scale). The dotted curve at the top shows the calculated plot obtained under the assumption that no change in the electronic configuration takes place in the  $\text{Ce}_\gamma - \text{Ce}_\alpha$  compression (left-hand ordinate scale).

cerium. The  $\gamma$  cerium (configurations  $4f^{0.9-1}5d^{1-1.1}6s^2$ ) turns out to be unstable. The negative pressure of the  $\text{Ce}_\gamma - \text{Ce}_\alpha$  transition (the slope of the common tangent to the  $4f^{0.4}5d^{1.6}6s^2$  and  $4f^{0.9}5d^{1.1}6s^2$  curves, corresponding closest to the experimental valences), turns out to be 50 kbar, corresponding in order of magnitude to extrapolation to  $T = 0^\circ\text{K}$  of the experimental  $\text{Ce}_\gamma - \text{Ce}_\alpha$  boundary on the  $pT$  phase diagram of cerium ( $p \approx 20$  kbar, see Fig. 2). The relative change in the volumes corresponding to the minima of the  $\alpha$  and  $\gamma$  curves is 16%, in good agreement with the experimental  $\Delta V/V \approx 17\%$ . The absolute values of the calculated  $\text{Ce}_\gamma$  and  $\text{Ce}_\alpha$  radii exceed the experimental ones by 12%. The still more compressed configuration  $5d^2 6s^2$ , which has no 4f electrons at all, can correspond to the  $\alpha'$  cerium which was recently observed experimentally<sup>[14]</sup> (see Fig. 2).

The fractional configurations can be regarded as a resonance of the Pauling type between the whole-number states  $4f^1 5d^1 6s^2$  and  $4f^0 5d^2 6s^2$ , corresponding to the  $\gamma$  and  $\alpha'$  phases. The resonant configuration set in correspondence with the  $\alpha$  cerium, which is stable at low temperatures (and gives an absolute minimum of  $E_\Sigma$  at a volume  $V^*$  close to the region of intersection of the  $\gamma$  and  $\alpha'$  curves) should in this case be written in the form  $4f^{0.5} 5d^{1.5} 6s^2$ , i.e., it should contain 0.5 of a 4f electron.

The energy differences between the K lines, calculated from relation (4) at the points of the minima of curves  $\alpha$  and  $\gamma$  (which differ by 0.5 4f electron), are given in Table V (first line). The obtained dependence of the shift on the type of line can be directly compared with the experimental one for  $\alpha - \gamma$  cerium (Fig. 6), and also with the previously calculated and experimentally measured dependence for  $\text{Ce}^{\text{III}} - \text{Ce}^{\text{IV}}$  (Fig. 8). These quantities are also given in Table V. The comparison can be made in the following manner. We obtain the ratios of the experimental and calculated shifts for trivalent and tetravalent cerium. They are

TABLE V. Comparison of experimental and calculated shifts of x-ray lines for  $\text{Ce}_\gamma - \text{Ce}_\alpha$  transition and for the chemical compounds  $\text{Ce}^{\text{III}}$  and  $\text{Ce}^{\text{IV}}$

No.	Discussed relations	Values of the shift $\Delta E$ (meV) and the ratios $\xi$ and $\eta$		
		$K_{\alpha_1}$	$K_{\beta_1}$	$K_{\beta_{3,4}}$
1	$\Delta E_{\text{Ce}_\gamma - \text{Ce}_\alpha}$ Calculation with WS boundary conditions	-410	-1140	-390
2	$\Delta E_{\text{Ce}_\gamma - \text{Ce}_\alpha}$ Experiment at low temperature	$-173 \pm 14$	$-566 \pm 32$	$-103 \pm 73$
3	$\Delta E_{\text{Ce}^{\text{III}} - \text{Ce}^{\text{IV}}}$ Calculation with boundary conditions at infinity	-746	-2200	-720
4	$\Delta E_{\text{Ce}^{\text{III}} - \text{Ce}^{\text{IV}}}$ Experiment with chemical compounds	$-300 \pm 20$	$-1150 \pm 40$	$-390 \pm 120$
5	$\xi \equiv \frac{\Delta E_{\text{Ce}^{\text{III}} - \text{Ce}^{\text{IV}}} \text{ exp.}}{\Delta E_{\text{Ce}^{\text{III}} - \text{Ce}^{\text{IV}}} \text{ calc}}$	0.40	0.52	0.54
6	$\Delta E_{\text{Ce}_\gamma - \text{Ce}_\alpha} \text{ calc} \cdot \bar{\xi}$	-197	-547	-187
7	$\eta \equiv \frac{\Delta E_{\text{Ce}_\gamma - \text{Ce}_\alpha} \text{ exp}}{\Delta E_{\text{Ce}^{\text{III}} - \text{Ce}^{\text{IV}}} \text{ calc}}$	$0.58 \pm 0.06$	$0.49 \pm 0.03$	$0.26 \pm 0.20$
8	Shifts corresponding to compression as in $\text{Ce}_\gamma - \text{Ce}_\alpha$ transition, but under the assumption that the number of 4f electrons remains unchanged (calculation with WS boundary conditions)	-50	-115	-200

given in Table V (line 5). The weighted average value  $\bar{\xi} = 0.48 \pm 0.04$  is quite close to the value  $\bar{\xi} = 0.46$  obtained in the analogous case for  $\text{Pr}^{\text{III}} - \text{Pr}^{\text{IV}}$  in<sup>[31]</sup>. Assuming that the difference between  $\xi$  and unity is due to some general defect of the theory, we introduce it in the form of a normalizing (scale) factor into the calculated values for  $\text{Ce}_\gamma - \text{Ce}_\alpha$  (Table V, line 1). These values, multiplied by  $\bar{\xi}$ , are given in Table V (line 6); they agree quite well with the data of the low-temperature experiment (Table V, line 2).

The experimental values for  $\text{Ce}^{\text{III}} - \text{Ce}^{\text{IV}}$  and the calculated values for  $\text{Ce}^{\text{III}} - \text{Ce}^{\text{IV}}$  ( $\text{C}_{4f} - \text{C}_{5d}$ , obtained with boundary conditions at infinity), normalized to the experimental ones with the definition of  $\bar{\xi}$ , the experimental (low-temperature) values for  $\text{Ce}_\gamma - \text{Ce}_\alpha$ , and, finally, the calculated values for  $\text{Ce}_\gamma - \text{Ce}_\alpha$  ( $(\text{C}_{4f} - \text{C}_{5d})/2$  with the WS boundary conditions), corrected by multiplication by  $\bar{\xi}$ , are shown in Fig. 10.

Table V (line 7) shows the ratios  $\eta$  of the experimental  $\text{Ce}_\gamma - \text{Ce}_\alpha$  and experimental  $\text{Ce}^{\text{III}} - \text{Ce}^{\text{IV}}$  shifts for individual lines and the weighted average value  $\bar{\eta}$ , which obviously gives the fractional change in the number of 4f electrons in the low-temperature  $\text{Ce}_\gamma - \text{Ce}_\alpha$  transition in comparison with the change occurring on going from trivalent to tetravalent cerium compounds.

It is very important to estimate the effect that would take place if the  $\text{Ce}_\gamma - \text{Ce}_\alpha$  transition were not accompanied by a change in the number of 4f electrons. This can be done by calculating the K-line energy differences for any specified (constant) configuration at WS-sphere volumes corresponding to the experimental ones for  $\gamma$  and  $\alpha$  cerium. These data, calculated for the configuration  $4f^1 5d^1 6s^2$  are given in Table V (line 8) and in Fig. 10 (top); they remain in force, accurate to 10%, also for other configurations<sup>3)</sup>.

## DISCUSSION OF RESULTS AND CONCLUSIONS

The experimental shift of the K lines in the  $\text{Ce}_\gamma - \text{Ce}_\alpha$  transition are analogous in sign, absolute values, and

the characteristic V-shaped dependence on the type of line to the shifts observed between compounds of trivalent and tetravalent cerium (Figs. 8 and 10). The latter are due to an effect that has by now been well investigated (see, in particular, <sup>[16,27,31,32]</sup>), namely the change of the number of 4f electrons in rare-earth elements with variable valence<sup>4)</sup>.

The shifts due to processes in which electrons with other values of  $l$  take part ( $s$ ,  $p$ , and  $d$  electrons) are smaller by approximately one order of magnitude in absolute value and cannot imitate the observed shifts (see top of Fig. 1, as well as <sup>[16]</sup>). If it is assumed that in the case of Ce<sup>III</sup>-Ce<sup>IV</sup> the effect is due to a complete transition of one 4f electron of Ce<sup>III</sup> to one of the valence levels, then we can conclude from a comparison of the absolute values of the experimental shifts for the low-temperature Ce <sub>$\gamma$</sub> -Ce <sub>$\alpha$</sub>  transition and the Ce<sup>III</sup>-Ce<sup>IV</sup> transition that the Ce <sub>$\gamma$</sub> -Ce <sub>$\alpha$</sub>  transformation involves a decrease in the number of collapsed 4f electrons of  $\gamma$  cerium by an approximate average of 1/2 electron per atom (Table 5, line 7).

As expected, the 4f-5d transition in cerium has been observed in "compressed" Laves phases of CeFe<sub>2</sub>, CeCo<sub>2</sub>, and CeNi<sub>2</sub> (see Table III and Fig. 8). The results agree with the qualitative conclusions of studies in which it was concluded, on the basis of an analysis of the experimental data on the lattice constants <sup>[33,34]</sup> and measurements of the magnetic susceptibility <sup>[35-37]</sup> of the Laves phases, that 4f-5d transitions are present in CeF<sub>2</sub>, CeCo<sub>2</sub>, and CeNi<sub>2</sub>, but are absent in CeMg<sub>2</sub> and CeAl<sub>2</sub>. However, the fractions of 4f-5d transitions in CeFe<sub>2</sub>, CeCo<sub>2</sub>, and CeNi<sub>2</sub> (see the values of  $\eta$  in Table III) are somewhat smaller than expected (we expected  $\eta \gtrsim 0.5$ ) and differ noticeably from one another. The explanation may lie in the properties of the final state of the transition from 4f to the valence band, which is located near the Fermi level determined by the common aggregate of the conduction electrons of the lattice, and therefore depends significantly on the second partners in the Laves phases.

The mechanism based on the change in the number of 4f electrons is also confirmed by the results of theoretical calculations, in which the characteristic displacement vs. line type curves are well reproduced. Calculation can also yield a very good description of the situation as a whole (see Fig. 9); this appears to be an independent confirmation of the correctness of the assumed model of the effect. It is important that a change of volume without a change of the electronic configuration yields, for any of the conceivable configurations, an effect that is smaller by several times than the experimental one, and with a different form of the dependence on the type of line (Fig. 10, top, and Table V, line 8). It is therefore totally impossible to explain the observed changes in the energies of the K lines with the framework of interactions accounted for by the Hartree-Fock method, without assuming the 4f-5d transition.

The obtained proofs that the number of 4f electrons is decreased by approximately one-half in the Ce <sub>$\gamma$</sub> -Ce <sub>$\alpha$</sub>  transition are quite unambiguous. Thus, the interpretation of results of investigations with positron annihilation<sup>[9-11]</sup> (see the Introduction) is apparently in error. The probable cause is mentioned by the authors of these papers themselves and is analogous to the narrowing of the angular distribution of  $\gamma$  quanta and the increase of

the lifetimes of the positrons in a plastically deformed sample. The point, however, is not only and not so much the presence and magnitude of the plastic deformation itself, as the defects (vacancies) that are produced thereby. The investigated Ce <sub>$\gamma$</sub> -Ce <sub>$\alpha$</sub>  transition is connected with a 17% reduction in the volume of the produced  $\alpha$  phase, and it would therefore be accompanied by the appearance of defects around the nuclei of the  $\alpha$  phase in the parent lattice of the  $\gamma$  phase, and accordingly by an increase in the lifetimes of the positrons and a narrowing of the angular distribution of the  $\gamma$  quanta. These effects are the opposite of those expected in the 4f-5d transition, and apparently offset them to a considerable degree in the annihilation experiment.

The authors thank A. I. Smirnov and G. P. Solodov for taking part in constructing the experimental installation, A. I. Egorov for preparing the cerium compounds, V. K. Nikulin for useful discussions, Yu. I. Vasil'ev and B. V. Kokarev for help in preparing the instrument and with the measurement.

We also wish to thank Corresponding Member of the USSR Academy of Sciences E. M. Savitskiĭ and Doctor of Technical Sciences V. F. Terekhov for consultations during the preparation of the Laves phases.

<sup>1)</sup>The shift  $\Delta E$  is much smaller than the line width  $\Delta$  (in our case  $\Delta E/\Delta \approx 1/50$ ). The shift of the summary line should be proportional to the intensity of the shifted component, i.e., to the concentration of the  $\alpha$  phase.

<sup>2)</sup>It should be noted that this assumption does not play a decisive role in the calculation of  $\eta$ . Any other assumption concerning the subsequent fate of the 4f electron will not change the value of  $\eta$  by more than 10-15%. The reason is that the shifts produced upon removal of a 4f electron are larger by approximately one order of magnitude than the shift produced upon removal (addition) of valence electrons of any other symmetry.

<sup>3)</sup>In <sup>[6]</sup>, in a calculation analogous to that described above, somewhat different boundary conditions were used:

$$\begin{aligned} f(r)|_{r=R_{WS}} &= 0 \text{ for } l \text{ even,} \\ g(r)|_{r=R_{WS}} &= 0 \text{ for } l \text{ odd.} \end{aligned} \quad (7)$$

The absolute minimum of  $E_{\Sigma}$  (see Fig. 9) corresponds in this case to the configuration 4f<sup>1</sup>5d<sup>1</sup>6s<sup>2</sup>, i.e., at  $T = 0^\circ\text{K}$  the predicted stable cerium modification is  $\gamma$  and not  $\alpha$ . The conditions (7) seem to us, however, to be unphysical, calling for a discontinuity in the derivative of the electron density on the WS sphere, i.e., at the midpoint of the distance between neighboring atoms. Unfortunately, the results of Fig. 9 also depend significantly on the choice of the constant  $C$  in the relation for the exchange potential. Thus, at  $C = 2/3$  the absolute minimum corresponds to  $\alpha$  cerium also under conditions (7); under our boundary conditions and at  $C = 2/3$ , the  $\alpha$  cerium is already excessively stable. The character of the plots of the shift against the line types remains practically the same for all these variants, and only a relatively small ( $\leq 30\%$ ) change in the absolute values of the shifts is observed.

<sup>4)</sup>In addition to the data shown in Figs. 1 and 10 for  $\text{Pu}$ ,  $\text{Sm}$ , and  $\text{Ce}$ , analogous shifts were also observed for  $\text{Yb}^{\text{II}} - \text{Yb}^{\text{III}}$ ,  $\text{Tb}^{\text{III}} - \text{Tb}^{\text{IV}}$  <sup>[27]</sup>, and  $\text{Pr}^{\text{III}} = \text{Pr}^{\text{IV}}$  <sup>[27, 31]</sup>.

<sup>1)</sup>P. W. Bridgman, Proc. Amer. Acad. Arts Sci. 58, 166 (1923).

<sup>2)</sup>F. Trombe, C. R. Acad. Sci., Paris 198, 1591 (1934).

<sup>3)</sup>K. A. Gschneidner, Splay redkozemel'nykh metallov (Alloys of Rare-Earth Metals) (Russ. Transl.), IIL, 1965.

<sup>4)</sup>W. H. Zachariasen, Phys. Rev. 76, 301 (1949).

<sup>5)</sup>L. Pauling, J. Chem. Phys. 18, 145 (1950).

<sup>6)</sup>J. T. Waber, D. Liberman, and D. T. Cromer, Proc. of the Conf. on Rare-Earth Research, Phoenix, Arizona, ed. by Eyring, N.Y., 1965.

- <sup>7</sup>V. L. Pokrovskii and G. V. Uimin, Zh. Eksp. Teor. Fiz. **55**, 1555 (1968) [Sov. Phys.-JETP **28**, 814 (1969)].
- <sup>8</sup>R. Ramires and L. M. Falicov, Phys. Rev. **3B**, 2425 (1971).
- <sup>9</sup>D. R. Gustafson and A. R. Mackintosh, J. Phys. Chem. Sol. **25**, 389 (1964).
- <sup>10</sup>D. R. Gustafson, J. D. McNutt, and L. O. Roellig, Phys. Rev. **183**, 435 (1969).
- <sup>11</sup>R. F. Gempel, D. R. Gustafson, and J. D. Willenberg, Phys. Rev. **5B**, 2082 (1972).
- <sup>12</sup>S. Kahana, Phys. Rev. **129**, 1622 (1963).
- <sup>13</sup>B. Coqblin and A. Blandin, Advan. Phys. **17**, 281 (1968).
- <sup>14</sup>E. King, J. A. Lee, I. R. Harris, and T. F. Smith, Phys. Rev. **1B**, 1380 (1970).
- <sup>15</sup>O. I. Sumbaev, Zh. Eksp. Teor. Fiz. **57**, 1716 (1969) [Sov. Phys.-JETP **30**, 927 (1970)].
- <sup>16</sup>E. V. Petrovich, Yu. P. Smirnov, V. S. Zykov, A. I. Grushko, O. I. Sumbaev, I. M. Band, and M. B. Trzhaskovskaya, Zh. Eksp. Teor. Fiz. **61**, 1756 (1971) [Sov. Phys.-JETP **34**, 935 (1972)].
- <sup>17</sup>I. M. Band and M. B. Trzhaskovskaya, Tablitsa sobstvennykh znacheniĭ energii elektronov, plotnostei v nule i srednikh znacheniĭ v samosoglasovannykh polyakh atomov i ionov,  $37 \leq Z \leq 64$  (Table of Eigenvalues of Electron Energy, Density at Zero, and Mean Values in Self-Consistent Fields of Atoms and Ions,  $37 \leq Z \leq 64$ ), Leningrad, A. F. Ioffe, Physico-technical Institute, USSR Acad. Sci., 1971.
- <sup>18</sup>O. I. Sumbaev, Zh. Eksp. Teor. Fiz. **54**, 1352 (1968) [Sov. Phys.-JETP **27**, 724 (1968)].
- <sup>19</sup>A. I. Smirnov, V. A. Shaburov, V. L. Alekseyev, D. M. Kaminker, A. S. Rylnikov, and O. I. Sumbaev, Nucl. Instr. and Meth. **60**, 103 (1968).
- <sup>20</sup>O. I. Sumbaev and A. F. Mezentsev, Zh. Eksp. Teor. Fiz. **49**, 459 (1965) [Sov. Phys.-JETP **22**, 323 (1966)].
- <sup>21</sup>C. J. McHarque and H. L. Yakel, Acta. Met. **8**, 637 (1960).
- <sup>22</sup>M. K. Wilkinson, H. R. Child, and C. J. McHarque, Phys. Rev. **122**, 1409 (1961).
- <sup>23</sup>K. A. Gschneidner, Jr., R. O. Elliott, and R. R. McDonald, J. Phys. Chem. Sol. **23**, 555 (1962).
- <sup>24</sup>M. E. Teslyuk, Metallicheskie soedineniya so strukturami faz Lavesa (Metallic Compounds with Laves Phase Structure), Nauka, 1969.
- <sup>25</sup>E. Franceschi and G. L. Olcese, Phys. Rev. Lett. **22**, 1299 (1969).
- <sup>26</sup>M. V. Nevitt, translation in :Elektronnaya struktura perekhodnykh metallov i khimiya ikh splavov (Electronic Structure of Transition Metals and the Chemistry of their Alloys), IIL, 1966.
- <sup>27</sup>Yu. P. Smirnov, O. I. Sumbaev, E. V. Petrovich, V. S. Zykov, A. I. Egorov, and A. I. Grushko, Zh. Eksp. Teor. Fiz. **57**, 1139 (1969) [Sov. Phys.-JETP **30**, 622 (1970)].
- <sup>28</sup>J. C. Slater, Phys. Rev. **81**, 385 (1951).
- <sup>29</sup>R. Latter, Phys. Rev. **99**, 510 (1955).
- <sup>30</sup>T. C. Tucker, L. D. Roberts, C. W. Nestor, Jr., T. A. Carlson, and F. B. Malik, Phys. Rev. **178**, 998 (1969).
- <sup>31</sup>P. L. Lee, E. S. Seltzer, and F. Boehm, Phys. Lett. **38A**, 29 (1972).
- <sup>32</sup>O. I. Sumbaev, Yu. P. Smirnov, E. V. Petrovich, V. S. Zykov, and A. I. Grushko, ZhETF Pis. Red. **10**, 209 (1969) [Sov. Phys.-JETP Lett. **10**, 131 (1969)].
- <sup>33</sup>I. R. Harris, R. C. Mansey, and G. V. Raynor, J. Less-Common Met., **9**, 270 (1965).
- <sup>34</sup>I. R. Harris and R. C. Mansey, J. Less-Common Met., **13**, 591 (1967).
- <sup>35</sup>E. A. Skrabek, and W. E. Wallace, J. Appl. Phys. **34**, 1356 (1963).
- <sup>36</sup>J. W. Ross and J. Grangle, Phys. Rev. **133A**, 509 (1964).
- <sup>37</sup>G. K. Wertheim and I. H. Wernick, Phys. Rev. **125**, 1937 (1962).

Translated by J. G. Adashko  
117